

Geophysical and geotechnical assessment of a railway embankment failure

Donohue, S., Gavin, K., & Tolooiyan, A. (2011). Geophysical and geotechnical assessment of a railway embankment failure. *Near Surface Geophysics*, 9(1), 33-44. <https://doi.org/10.3997/1873-0604.2010040>

Published in:
Near Surface Geophysics

Document Version:
Peer reviewed version

Queen's University Belfast - Research Portal:
[Link to publication record in Queen's University Belfast Research Portal](#)

General rights

Copyright for the publications made accessible via the Queen's University Belfast Research Portal is retained by the author(s) and / or other copyright owners and it is a condition of accessing these publications that users recognise and abide by the legal requirements associated with these rights.

Take down policy

The Research Portal is Queen's institutional repository that provides access to Queen's research output. Every effort has been made to ensure that content in the Research Portal does not infringe any person's rights, or applicable UK laws. If you discover content in the Research Portal that you believe breaches copyright or violates any law, please contact openaccess@qub.ac.uk.

Geophysical and geotechnical assessment of a railway embankment failure

Shane Donohue*, Kenneth Gavin and Ali Tolooiyan

School of Architecture, Landscape and Civil Engineering, University College Dublin (UCD), Newstead, Belfield, Dublin 4, Ireland

Received July 2009, revision accepted July 2010

ABSTRACT

A geophysical investigation was carried out after the failure of an important railway embankment in the south-east of Ireland. The embankment, which had a long-term history of stability problems, was studied using a combination of ground-penetrating radar (GPR), electrical resistivity tomography (ERT), multichannel analysis of surface waves (MASW) and geotechnical testing. A significant thickening of the ballast layer around the failure location was observed using GPR, which confirmed the existence of an ongoing stability problem in the area. ERT profiles determined the presence and spatial extent of a significant layer of soft clay both beneath and to the east of the embankment, which could have a major impact on its long-term stability. ERT also detected steeply sloping bedrock close to the failure zone that is likely to have contributed to the long-term settlement of the embankment, which necessitated frequent re-ballasting. MASW confirmed the presence of the steeply sloping bedrock in addition to determining the low stiffness (G_{\max}) values of the embankment fill.

High quality sampling of the soft clay deposit was undertaken and strength and compressibility tests revealed the importance of this layer to both the on-going serviceability problems evident for the original embankment and the stability problems encountered by the remodelled section.

INTRODUCTION

Since the early work of Bogoslovsky and Ogilvy (1977) and McCann and Forster (1990), geophysical techniques have been used increasingly in landslide and slope stability investigations (e.g., Hack 2000; Cosentino *et al.* 2003; Jongmans and Garambois 2007). Geophysical techniques are well-suited for these studies as they may provide information on subsurface geology and hydrogeology. Furthermore, a number of these techniques are non-invasive and cost-effective, which make them ideal for studying the spatial and temporal variations of the subsurface that cannot be captured using discrete boreholes or other forms of geotechnical investigation. Geophysical methods are therefore ideally used as a complementary tool, which, together with traditional geotechnical investigations, will typically provide a more complete understanding of the physical behaviour of the slope or landslide in question.

A number of different geophysical methods have been used recently to investigate soil, rock and groundwater conditions in areas susceptible to landslides. These include electrical (e.g., Suzuki and Higashi 2001; Lapenna *et al.* 2003; Friedel *et al.* 2006; Mondal *et al.* 2008), electromagnetic (e.g., Schmutz *et al.* 2000) and seismic (e.g., Rix and Stokoe 1988; Deidda and Ranieri 2005) methods. A number of authors have shown that the reliability of a geophysical investigation may be considerably improved by using several techniques on site (e.g., Caris and Van

Asch 1991; Godio and Bottino 2001; Göktürkler *et al.* 2008).

This paper describes an investigation into the recent failure of a railway embankment near Enniscorthy in the south-east of Ireland (Fig. 1). The embankment, which was built in the 1850s, had experienced long-term settlement problems that resulted in the need to frequently reballast the line. Because of these ongoing problems and a requirement to increase the shoulder width of the top of the embankment, the line was selected for remodelling. These works involved the construction of a full height reinforced berm, made up of ballast fill on the River Slaney side of the existing embankment (see Fig. 1). In December 2006, during remodelling works, a major slope failure occurred. An investigation was commissioned to determine the cause of the failure, the first phase of which consisted of drilling four, shell and auger boreholes perpendicular to the failure surface (see Fig. 1). This was followed by a geophysical investigation, sampling and laboratory testing, which are described in detail in this paper. The range of geophysical techniques used, included ground-penetrating radar (GPR), electrical resistivity tomography (ERT) and multichannel analysis of surface waves (MASW).

STUDY AREA

Background information

The development of the Irish railway network in the 1850s involved the construction of a large number of man-made slopes, both cutting and fills, in the glacial soils that cover much of the

* shane.donohue@ucd.ie

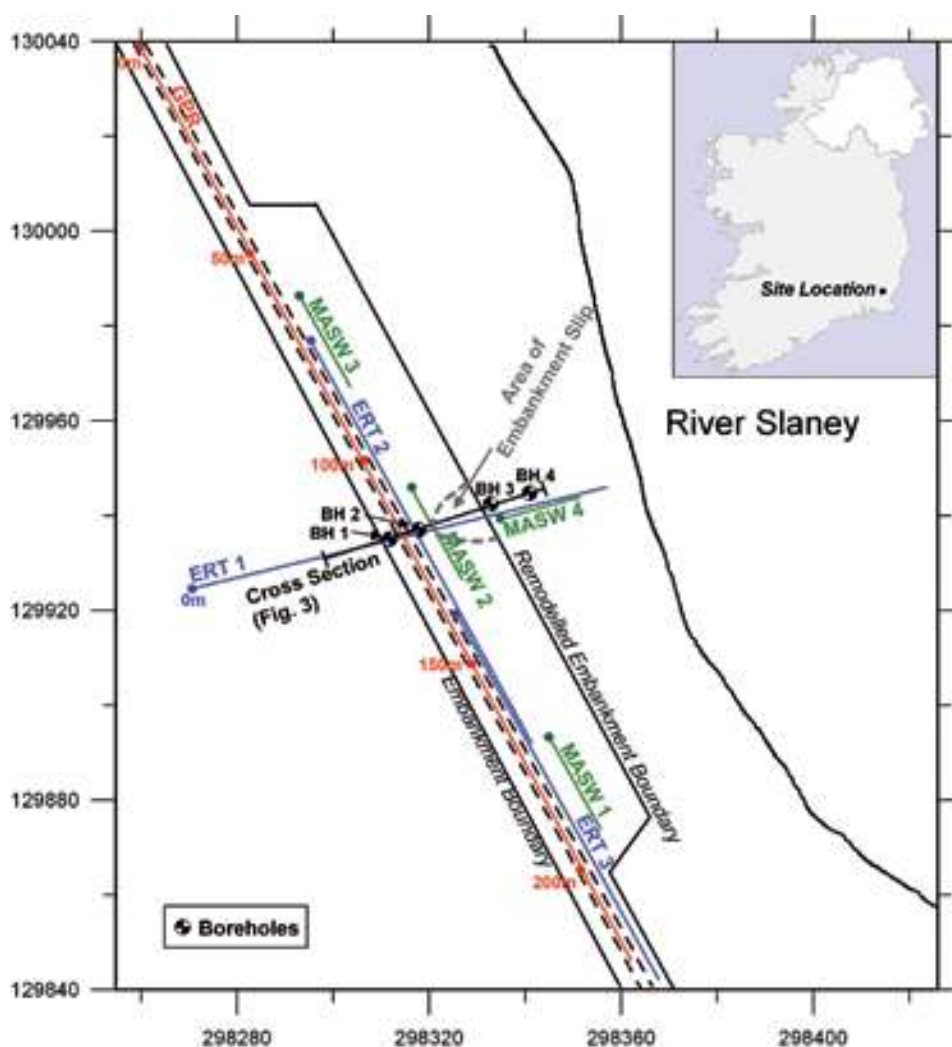


FIGURE 1

Location of GPR, ERT and MASW geophysical investigations along with boreholes carried out at the site of the railway embankment failure. The site is located in Co. Wexford in the south-east of Ireland (inset).

country. A recent inventory of fill slopes formed in glacial soils (Gavin *et al.* 2006) revealed slope angles in the range 24° – 60° , with 90% of the slopes having a slope angle greater than 30° . Current design practice for motorway networks in Ireland provides for a maximum slope angle of 27° in these soils. Due to displacements caused by seasonal wetting and drying cycles, strain softening has been identified as a trigger for delayed failure of slopes with similar geometry in London Clay (Kovacevic *et al.* 2001). With the notable exception of a marine till known as Macamore Clay (Doherty *et al.* 2006) most glacial soils encountered in Ireland do not exhibit strain-softening behaviour and despite their high slope angles, failure rates are relatively low (typically one to two per year). These slips tend to be shallow (<1 m deep) translational failures commonly associated with rainfall infiltration. As the soil at or near formation level is usually strong intact glacial till, the slip surface tends not to propagate below the toe of the embankment and therefore only temporary disruption to the operation of the railway usually results. The effect of suction on the stability of steep slopes is well

understood (Fourie *et al.* 1999) and its contribution to the relative stability of the slopes in Irish glacial soils is discussed by Xue (2006). An important element in the repair of these minor failures is often confined to improving the slope drainage. However, given the possibility of future increased rainfall levels, there is some concern that the rate of shallow slope failures will increase in the coming years and a recent study to define these risks and to develop a programme of slope improvement works is underway at present by the network operator (Irish Rail). An integral part of this work is a back-analysis of failures to determine their failure mechanisms.

Site description

The railway embankment under investigation forms part of the main Dublin to Wexford railway line and is located near the town of Enniscorthy, adjacent to the River Slaney in the south-east of Ireland (Fig. 1). The local topography, considered perpendicular to the embankment, slopes towards the river and therefore the upgrade works were confined to the downslope (river) side,

where the original embankment height was 4 m and the slope angle varied from 45–68°. Because of land constraints, the remodelled embankment, which had a crest width of approximately 1 m was formed of ballast with geogrid reinforcement, which allowed a near vertical side slope to be formed. The remodelling work commenced in December 2006 and progressed well despite inclement weather. Although the months of October–December 2006 were unseasonably mild, the rainfall records taken at the nearest weather stations located in Kilkenny and Rosslare, shown in Fig. 2, reveal that the amount of rainfall was much higher than normal.

In mid-December a rotational slip occurred in the highly permeable upper ballast layer of a section of the embankment being remediated. The approximately circular failure surface developed on the river side of the embankment, beginning 800 mm from the edge of the crest and propagating less than one metre into the remediated section of the embankment. At the base, the slip extended approximately 1 m from the toe of the embankment. The works were halted immediately and a geotechnical investigation was arranged, the first stage of which involved drilling four shell and auger boreholes at the site of the slip (Fig. 3). The soil conditions encountered in the boreholes taken through the embankment suggested that the gravel ballast was over a metre deep at the crest (BH 2). No evidence of the slip surface was found in the boreholes. The embankment fill was described as being soft clay becoming soft to firm and this overlay a 2 m thick layer of stiff glacial till, which in turn overlay bedrock. Driller's logs described the bedrock as being weathered near the surface. The boreholes taken from the original ground surface (BH 4) revealed soft 'brown clay' overlying a layer of soft alluvial clay with occasional organic material to approximately 4 m below

ground level. Below this layer, a thin layer of stiff glacial till was found to overly weathered bedrock. To aid the forensic investigation of the slope failure a geophysical site investigation was carried out. The aims of this investigation were to supplement the information gained from the boreholes, in particular:

- to investigate the ballast thickness along the track.
- because there was some uncertainty regarding the actual depth to bedrock in the shell and auger boreholes (as boulders embedded in glacial till are often interpreted as bedrock), a profile of the top of bedrock was required.
- the soft clay revealed in all boreholes was of obvious interest and further information on the extent of this layer was critical to our understanding of the failure mechanism.

GEOPHYSICAL METHODS

Ground-penetrating radar (GPR)

Over the last number of years ground-penetrating radar (GPR) has been used by a number of authors for rapid and non-invasive monitoring of railway trackbed condition (Jack and Jackson 1999; Hugenschmidt 2000; Hyslip *et al.* 2003; Carpenter *et al.* 2004). These studies demonstrated the usefulness of GPR for determining the base of the important coarse-grained ballast layer. The open voids in clean ballast result in diffraction of the GPR pulse at the particle interfaces, which allows the ballast to be distinguished from the finer-grained sub-ballast layers (Hyslip *et al.* 2003). If the ballast layer has been fouled by the addition of fine-grained materials, GPR may also be used for determining the amount of fouling, as the finer particles will limit diffraction of the GPR pulse.

In this study the section of track under investigation (Fig. 1) was surveyed five times with different configurations of the GPR system, in order to optimize the resolution of the ballast horizon.

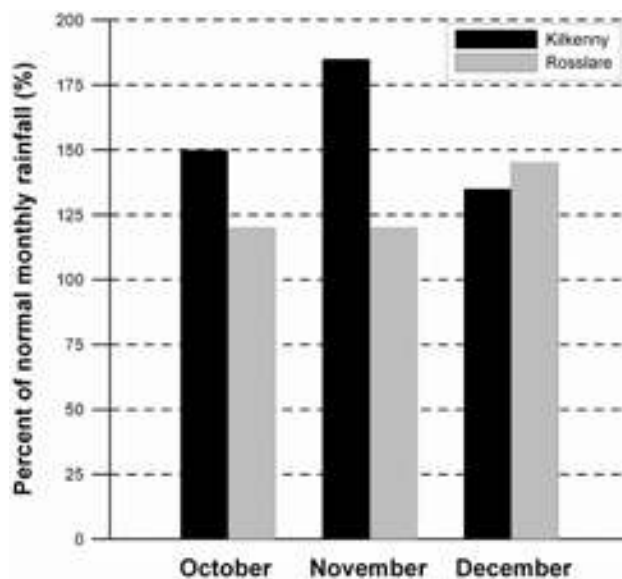


FIGURE 2

Rainfall records recorded in October, November and December 2006, at the Kilkenny and Rosslare weather stations in the south-east of Ireland.

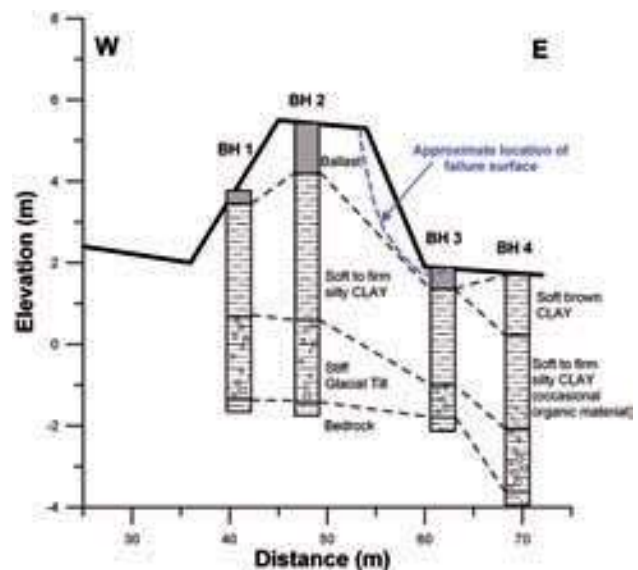


FIGURE 3

Borehole logs from the Enniscorthy railway embankment failure site.

The equipment used was a Monostatic (fixed transmitter-receiver offset) RAMAC system by Mala Geoscience of Sweden, with an 800 MHz ground coupled, shielded antenna used parallel to the profile direction (normal orientation). The transmitter-receiver spacing was 180 mm. Data collection was controlled with an electronic distance measuring wheel. Data were acquired both in step mode within each railway crib and in distance (continuous) mode, with traces recorded approximately every 20 mm. A number of processing steps were applied to the data including a time-zero adjustment, a Butterworth band-pass filter (220–1000 MHz) and an energy decay compensation (time variant gain). The time-zero adjustment was done by correction for maximum positive phase due to the transmitter, receiver offset. A 40-trace running average was also applied to the data collected in distance mode in order to remove the ringing effect of the railway sleepers. This was not required for the step mode data as the measurement was performed within each railway crib. The number of stacks performed on the step mode data was 4. A topographic correction was not required as the trackbed is flat in this area. In order to convert two-way traveltimes to depth a GPR velocity of 0.13 m/ns was used as this was found to represent an average velocity over a number of similar railway trackbed investigations (Hugenschmidt 2000; Carpenter *et al.* 2004).

Electrical resistivity tomography (ERT)

ERT is used to calculate the electrical resistivity distribution of the subsurface by measuring a large number of electrical potential differences for different combinations of surface electrodes. A number of authors have recently used resistivity measurements to investigate landslides and slope stability problems. These include investigations of the properties of the landslide body (e.g., Lapenna *et al.* 2003; Israil and Pachauri 2003; Göktürkler *et al.* 2008), location of the failure surfaces (e.g., Caris and Van Asch 1991; Godio and Bottino 2001; Göktürkler *et al.* 2008), landslide hazard assessments for active slides (e.g., Schmutz *et al.* 2000; Mondal *et al.* 2008) and investigation of the effects of rainfall infiltration (e.g., Caris and Van Asch 1991; Suzuki and Higashi 2001; Friedel *et al.* 2006).

ERT data for this project were acquired using a multi-electrode Campus Tigre resistivity meter with a 32 takeout multicore cable and 32 conventional stainless steel electrodes. A Wenner array configuration was used with an electrode spacing of 3 m. Data processing was carried out using the Res2Dinv software. This software uses a forward modelling subroutine to calculate the apparent resistivity values and a non-linear least-squares optimization technique is used for the inversion routine (deGroot-Hedlin and Constable 1990; Loke and Barker 1996).

The first profile (ERT 1) was acquired approximately perpendicularly across the track, through the failure zone (Fig. 1). The other profiles (ERT 2 and ERT 3) were both located parallel to the railway line along the crest of the embankment. Initially there was some concern that the ERT sections measured along the embankment crest would not be directly comparable to the per-

pendicular cross-section due to the effect of the embankment 3D topography (and of the air) on the measured resistivity values. This effect has been investigated by Shabi *et al.* (1997) and Sjødahl *et al.* (2006) and is discussed below.

Multichannel analysis of surface waves (MASW)

The use of surface waves for the estimation of shear-wave velocity (V_s) profiles has received considerable attention over the last number of years. The MASW method was first introduced in the late 1990s by Park *et al.* (1999) and Xia *et al.* (1999). As with the similar spectral analysis of the surface-waves (SASW) method (Nazarian and Stokoe 1984), the MASW method is concerned with shallow depths that are of interest to civil engineers. The most significant difference between the SASW and the MASW techniques, involves the use of multiple receivers with the MASW method (usually 12–60 receivers), which enable seismic data to be acquired relatively quickly when compared to the SASW method, which involves several measurements at different source-receiver configurations. Another advantage of the MASW approach is the ability of the technique to identify and separate fundamental and higher mode surface waves. According to elastic theory, the small strain shear modulus, G_{\max} , is related to V_s by the following equation:

$$G_{\max} = \rho V_s^2, \quad (1)$$

where G_{\max} = shear modulus (Pa), V_s = shear wave velocity (m/s) and ρ = density (kg/m^3).

The surface wave data for the Enniscorthy embankment site were recorded using a Geometrics Geode seismograph (with 24 geophones). A 10 kg sledgehammer was used to generate the sur-

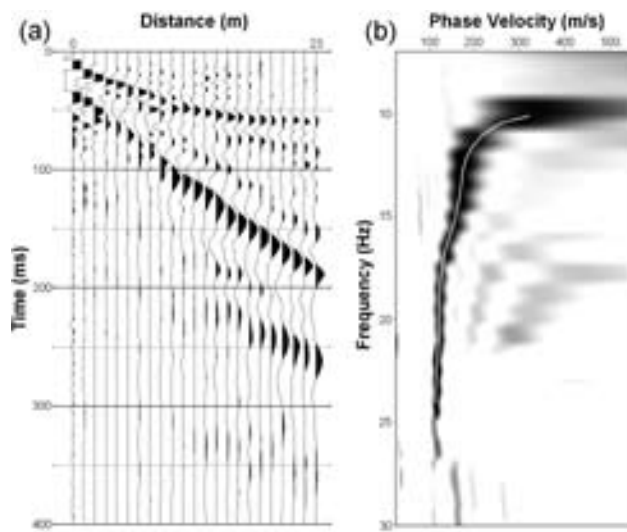


FIGURE 4

Example of a) a seismic shot gather and b) the corresponding picked dispersion curve (white line) from the phase velocity-frequency spectra for the multichannel analysis of surface waves profile MASW 1.

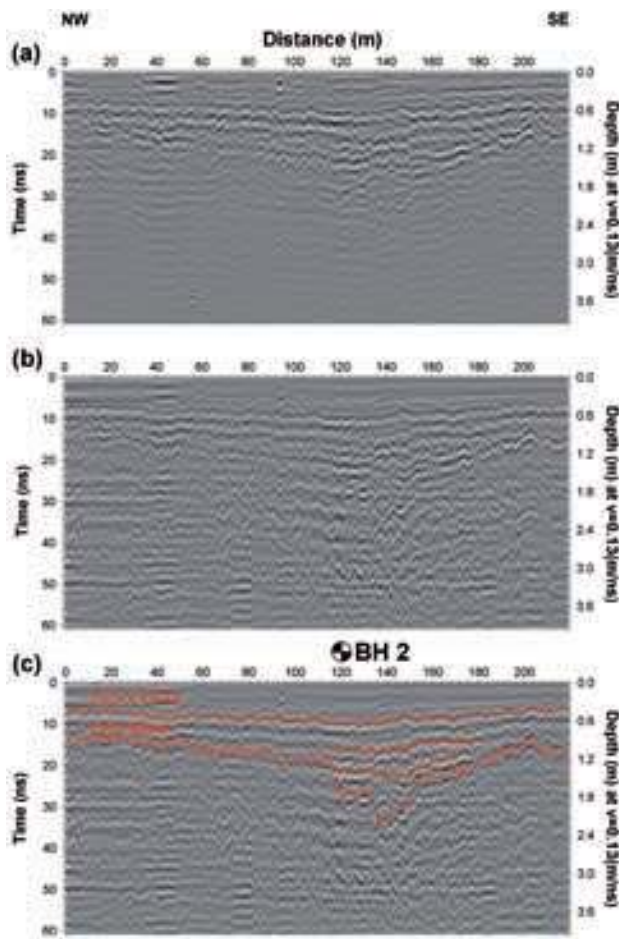


FIGURE 5

Processed GPR data recorded in a) step mode and b) distance mode. A GPR velocity of 0.13 m/ns was used to convert two-way traveltime to depth. An interpretation of the GPR section is shown in (c) with interpreted ballast boundaries shown in red. The deepest red line indicates the interpreted ballast base.

face waves, which were in turn detected by 10 Hz geophones at 1m intervals. Four MASW profiles were acquired, at various positions along the track (Fig. 1). These were located 1) south of the failure, parallel to the railway track, 2) directly over the failure plane, 3) north of the failure plane, also parallel to the track and 4) to the east of the embankment, towards the River Slaney. The software, Surfseis, was used to select a dispersion curve from the phase velocity-frequency spectra, which was generated using a wavefield transformation method (Park *et al.* 1998). An example of a seismic shot gather and the corresponding picked dispersion curve from the phase velocity-frequency spectra from this study is provided in Fig. 4. As shown, a normally dispersive phase velocity-frequency relationship was obtained that was dominated by the fundamental mode Raleigh wave. In this example the dispersion curve was picked over a frequency range of 10.5–24 Hz. 1D S-wave models were estimated by using the approach of Xia *et al.* (1999).

GEOPHYSICAL RESULTS

Ground-penetrating radar (GPR)

GPR data collected in step mode and in distance mode are illustrated in Fig. 5(a,b), respectively. Although there is some noise in both sections it is clear that the data recorded in step mode (one trace per crib, 346 traces in total) are less affected by noise. It should, however, be noted that the distance mode data, which contain approximately 12 500 traces, appear to have detected more detail. It is also far more practical in terms of acquisition speed and contains sufficient information to infer the ballast layer boundaries. An interpretation of the GPR data is provided in Fig. 5(c). A reasonably clear image of the base of the railway ballast interface is observed, together with reflections from the interfaces between subsequent phases of ballast layering. The base of the ballast was chosen as the last continuous boundary from the phase polarity, which because of the high-low velocity contrast between the ballast and subgrade layer results in a positive leading phase. The most recent surficial ballast layer is approximately 0.5–0.6 m thick and this is generally consistent throughout the length of the profile. Below this, however, the older ballast layer appears to considerably vary in thickness. The most interesting feature in the GPR profile occurs between 110–180 m where the ballast layer appears to thicken considerably over a very short distance to a depth of over 2 m. The presence of thicker ballast in this area suggests a long-term settlement problem, as ballast has clearly been continually added to this area in order to offset any settlement that may have occurred. The embankment failure also occurred in this area.

Electrical resistivity tomography (ERT)

Figure 6(a) shows the results of the electrical resistivity tomography survey, ERT1. The upper metre of the embankment contains a zone of very high resistivity ($>1000 \Omega\text{m}$), which corresponds to the layer of dry granular railway ballast observed in the GPR results. It is thought that the presence of this very high resistivity material could have insulated the electrodes from the metal rails, thereby negating their effect on the ERT profiles. Following comparison of this resistivity section with the borehole logs, shown in Fig. 3, an interpretation of this ERT profile is provided in Fig. 6(b). The very low resistivity signal ($<50 \Omega\text{m}$) lying directly below and to the east of the embankment is interpreted to be the soft alluvial clay material observed in boreholes BH3 and BH4. Below this layer the resistivity appears to gradually increase with depth. When comparing this data with the borehole information it appears that the layer of glacial till observed in the borehole logs would approximately correspond to a resistivity in the range of 50–150 Ωm , which is consistent with similar investigations in Irish glacial tills (O'Connor 2001). It should be noted, however, that the thin layer thickness of this deposit (approx. 2 m) relative to the electrode spacing (3 m) makes it difficult to accurately resolve. The illustrated interpretation of this layer (Fig. 6b), therefore, relies heavily on the borehole information. In Ireland, it is generally found that Irish gla-

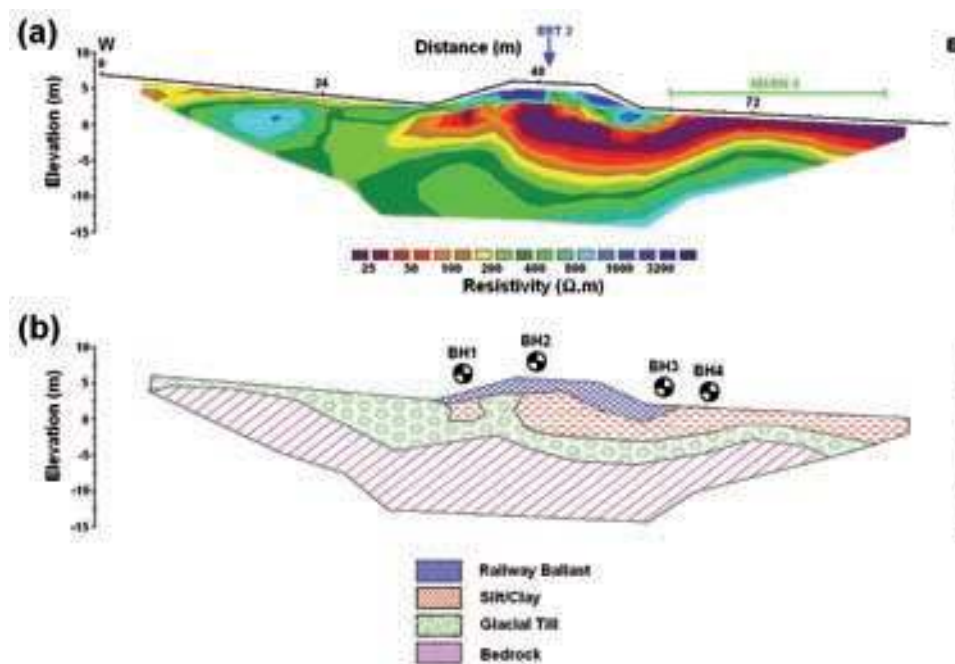


FIGURE 6

a) Inverted electrical resistivity tomography profile for ERT 1 (with rms error = 7.5 % after 5 iterations) and b) an interpretation, combining the resistivity results with the borehole cross-section shown in Fig. 3.

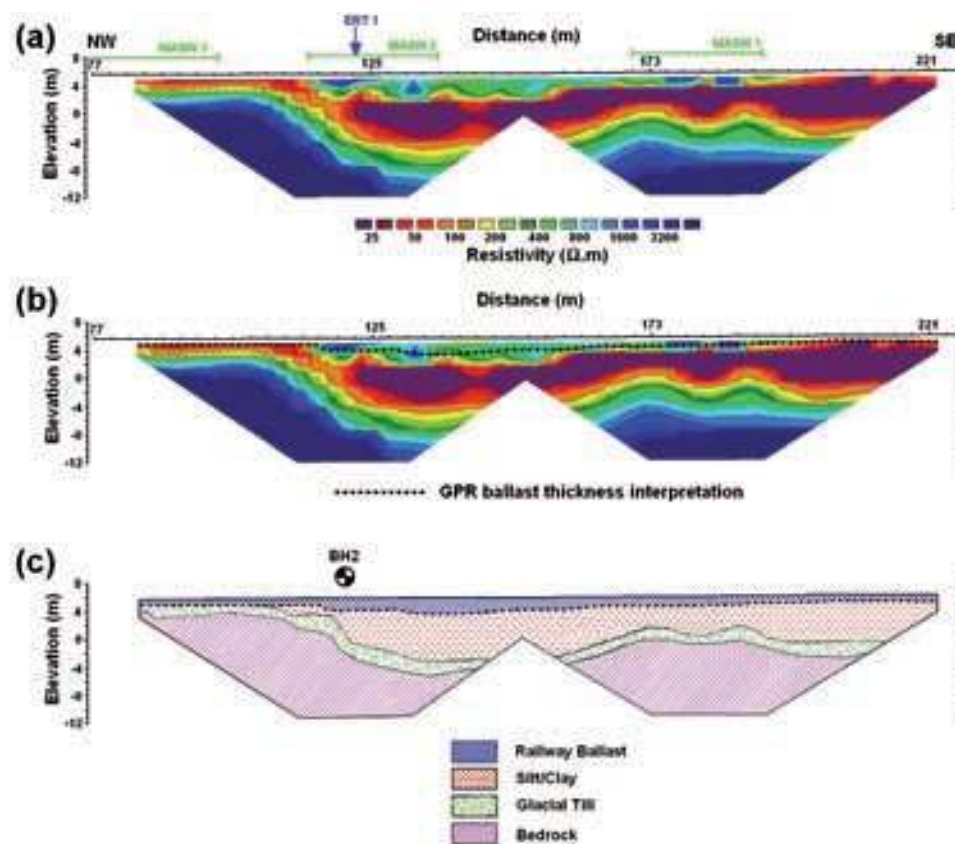


FIGURE 7

a) Inverted electrical resistivity tomography profile for the combined ERT 2 and ERT 3 (rms = 9.3 % after 5 iterations), b) with estimated ballast thickness from the GPR data (Fig. 5c) and c), an interpretation, combining the resistivity results with the borehole and GPR data.

cial till has a maximum resistivity of approximately 150 Ωm (O'Connor 2001). According to the borehole logs, this material is underlain by bedrock, therefore it is likely that this value approximately represents the interface between till and rock. The choice of this contour is also validated by comparison with most

of the borehole logs. There is a small discrepancy between the estimated depth to bedrock from borehole 3 and the ERT data, although it should be pointed out that there was some uncertainty regarding the actual depth to bedrock in this shell and auger borehole (boulders embedded in glacial till are often inter-

puted as bedrock). As shown, the bedrock appears to be shallower in the western / upslope side of the section.

A combined inversion of the collinear and overlapping profiles, ERT2 and ERT 3, was performed, the results of which are shown in Fig. 7(a). The very high resistivity ballast layer at the surface is not consistent over the entire section and appears to thicken significantly between 115–195 m of the profile. The railway ballast thickness, as estimated from the GPR data (Fig. 5c), is overlain on the inverted ERT profile in Fig. 7(b) for comparison purposes. As shown, the thicker layer of high resistivity material corresponds closely to the increase in ballast thickness interpreted from the GPR data. This layer, however, cannot be expected to be accurately resolved due to the relatively large electrode spacing (3 m) compared to the layer thickness (<2 m). Where the ballast is at its thickest (between 115–155 m) the ERT profile appears to overestimate the thickness.

An interpretation of this ERT profile combined with the GPR ballast interpretation is provided in Fig. 7(c). Bedrock, is again interpreted as a zone of high resistivity (>150 Ωm). As shown, the interpreted bedrock surface appears to dip steeply towards the south-east, between 110–125 m of the profile. The bedrock layer appears to dip from 3 m below the base of the embankment to 12 m at its deepest. This increase in bedrock depth is associated with a thickening of the low resistivity soft clay material and a corresponding thickening of the overlying ballast, as discussed above.

As shown in the captions of Figs 6 and 7, root-mean-square (rms) errors are relatively high (7.5% and 9.3%). This is thought to be due to the relatively poor signal-to-noise ratio observed

along the railway track. The slightly higher rms error for the combined profile (ERT2 and ERT3) is possibly due to the effect of the embankment 3D topography on the measured resistivity values. For ERT 1, which was oriented perpendicular to the railway, the embankment may be considered a 2D object. This 2D assumption is, however, violated for the profiles along the embankment crest, due to the effect of the embankment 3D topography (and of the air). This effect is discussed in detail by Shabi *et al.* (1997). As illustrated in the fence diagram (Fig. 8), both profiles appear to exhibit consistent resistivity values for most of the subsurface materials encountered. There is, however, a significant difference between the inverted resistivity of the bedrock on both profiles. The combined profile along the embankment crest (ERT 2 and ERT3) exhibits higher bedrock resistivity values (generally greater than 1600 Ωm) than ERT 1 and this is possibly due to the effect of the embankment 3D topography. It should be noted, however, that the interpreted bedrock surface (Fig. 7c) was consistent with the borehole information (BH2).

The ERT sections have identified a number of subsurface features that could have resulted in the long-term stability problems experienced by the embankment. Firstly, the presence and spatial extent of the very soft alluvial clay material below and to the east of the embankment (towards the river) in ERT1 could have had a major impact on the stability of the remodelled section of the embankment. Also, the steeply sloping bedrock in ERT2 together with the thicker zone of very soft clay are likely to have contributed to the long-term settlement issues at this location. This conclusion is also supported by the thicker layer of ballast detected around the failure location by both the ERT and

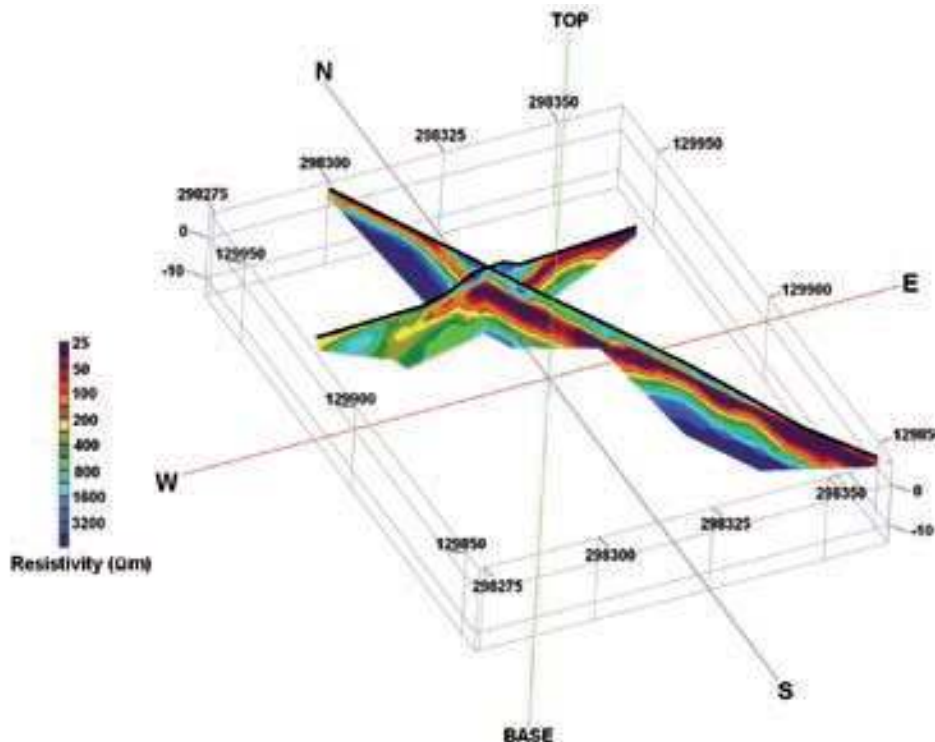


FIGURE 8

Fence diagram, combining ERT profiles, ERT 1 and ERT 2.

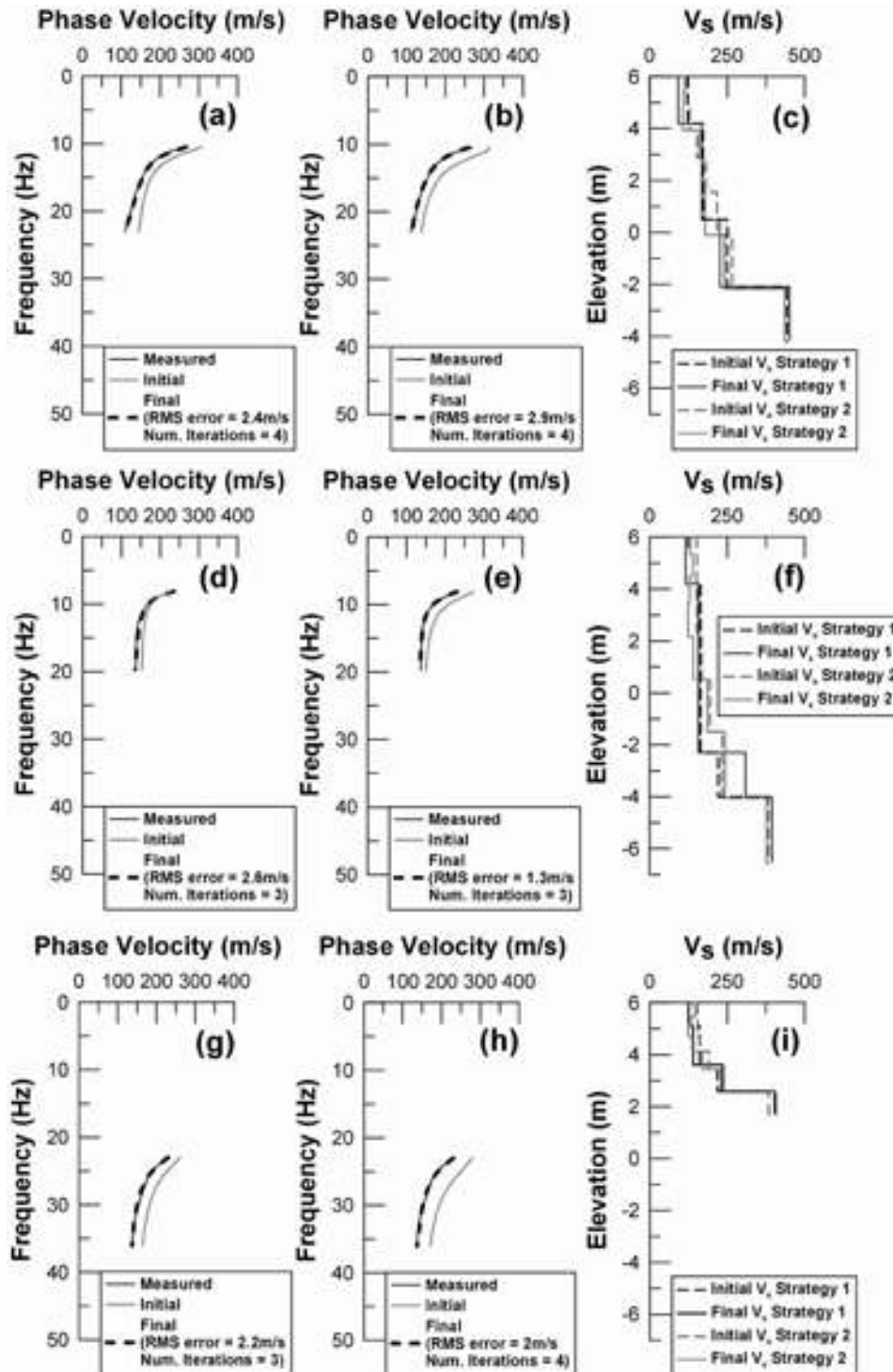


FIGURE 9

Measured, initial and final dispersion curves with associated errors for MASW 1 using a) inversion strategy 1, b) inversion strategy 2 and c) initial and final inverted MASW V_s profiles for MASW 1. Measured, initial and final dispersion curves with associated errors for MASW 2 using d) inversion strategy 1 and e) inversion strategy 2 and f) initial and final inverted MASW V_s profiles for MASW 2. Measured, initial and final dispersion curves with associated errors for MASW 3 using g) inversion strategy 1 and h) inversion strategy 2 and i) initial and final inverted MASW V_s profiles for MASW 3.

GPR profiles, which confirms that rebalasting of this area has been ongoing for some time, due to the settlement problems.

Multichannel analysis of surface waves (MASW)

Inversion of the measured dispersion curves was performed in two ways:

- 1 With the number of layers and layer thicknesses interpreted from the borehole and other geophysical data included as constraints in the initial model. A Poisson's ratio (ν) of 0.4 was used for all soil layers and $\nu = 0.25$ was used for the bedrock;
- 2 A number of different initial models with different numbers of layers were selected in the initial model in order to test the

robustness of the inversion and to determine the model with the lowest misfit. In order to reduce the non-uniqueness of the inversion, the borehole and other geophysical information are used to estimate the depth to bedrock and a Poisson's ratio (ν) of 0.4 was used for all soil layers and $\nu = 0.25$ was used for bedrock layers. Following the recommendations of Cercato (2009) and Luke and Calderón-Macías (2007) the layer thickness in the model was increased exponentially with depth. This reflects the fact that the resolving power of MASW data decreases with depth.

Initial, measured and final inverted surface wave dispersion curves and corresponding inverted V_s profiles, using both inversion strategies described above, for the MASW profiles located along the embankment crest (MASW 1, MASW 2 and MASW 3) are shown in Fig. 9. Each inversion was allowed a sufficient number of iterations to converge and was stopped after the rms error had levelled off. For dispersion curves inverted using the second inversion strategy, it was consistently found that an eight layer initial model produced the lowest rms error. Additional layers produced similar errors however, these resulted in over-parametrized inversions, as evidenced by inversion artefacts such as 'smoothing' over the layer boundaries as well as artefact low velocity layers, not supported by evidence from the local geology.

Inverted shear-wave velocity (V_s) profiles are illustrated in Figs 9(c), 9(f) and 9(i). Overall both inversion strategies resulted in very similar final V_s profiles for both MASW 1 (Fig. 9c) and MASW 3 (Fig. 9i). Some variation was, however, observed between the different inversion strategies applied to MASW 2 (Fig. 9f). This is possibly due to the constraint of having a very thick second layer (6.7 m) in the initial model using the first inversion strategy relative to the overall profile depth (12.5 m). Simple minimum layer geometries such as those used in the first inversion strategy may not be the most appropriate initial models to invert due to increasing effective confining stress (and therefore increasing V_s) within the subsurface layers themselves. Without this constraint in the initial model, the second inversion strategy converged to a significantly lower rms error (1.3 m/s, Fig. 9e) within the same number of iterations.

There were also significant differences observed in the inverted V_s profiles (and corresponding measured dispersion curves) from the different locations themselves. Higher velocities were observed following inversion of MASW 3 at significantly shall-

lower depths than either of the other profiles, which supports the findings from the ERT profiles. Inverted V_s profiles are overlain on the inverted ERT image from the embankment crest in Fig. 10, for comparison. As shown, the bedrock V_s values are quite low (400–500 m/s) and support the borehole interpretation of weathered bedrock, although these values are not uncommon in very stiff glacial tills in Ireland (Donohue *et al.* 2003). Also the shear-wave velocities measured for the embankment fill material were quite low (approx. 150 m/s) and correspond to a small strain stiffness, G_{\max} (equation (1)), of just 40 MPa (assuming a density of 1.8 Mg/m^3) indicating that the material is soft to firm.

Dispersion curves and corresponding inverted V_s profiles, obtained using both inversion strategies, for the MASW profile acquired on the natural ground to the east (MASW 4, see Fig. 1) are shown in Fig. 11. An eight layer initial model was again found to produce the lowest rms error using the second inversion strategy. Both inversion strategies, however, resulted in almost identical inverted V_s profiles. Very low V_s values (70–100 m/s) were measured for the upper 1.5 m, which correspond to a G_{\max} of approximately 10 MPa indicating a very soft material. This is thought to correspond to the soft brown clay observed in the borehole logs (Fig. 3). The V_s values for this deposit are similar to those reported for other Irish soft clays (50–150 m/s) reported by Donohue and Long (2008) and Donohue *et al.* (2004).

GEOTECHNICAL STABILITY OF EMBANKMENT

The initial geotechnical and subsequent geophysical investigations provided significant insight into the stratification of the soil and rock layers and suggested that the variable depth to bedrock and presence of a thick layer of soft clay may have had significant influence on the long-term settlement of the original embankment and stability problems that affected the remodelled section. The glacial soils in Ireland are relatively well characterized (Donohue and Long 2003; Long and Menkiti 2007; Gavin *et al.* 2008) and the greatest uncertainty concerned the engineering properties of the soft alluvial clay deposit. For this reason an additional, supplementary, intrusive site investigation was arranged to obtain high quality samples of this material for laboratory testing.

Additional site investigation

The geophysical and geotechnical investigations indicated that the soft clay layer existed near the ground surface in the vicinity

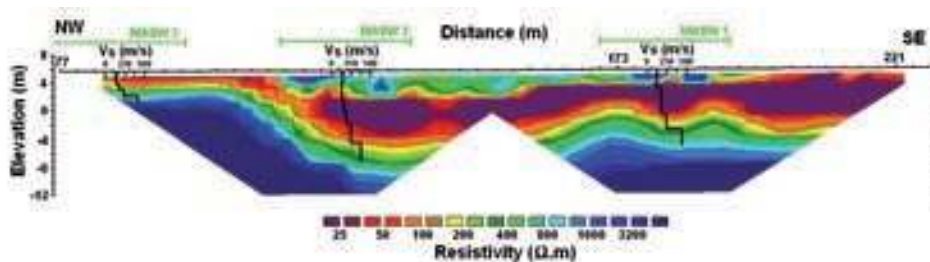


FIGURE 10
Inverted V_s profiles for MASW 1, MASW 2 and MASW 3 overlain on the inverted ERT cross-section from along the embankment crest.

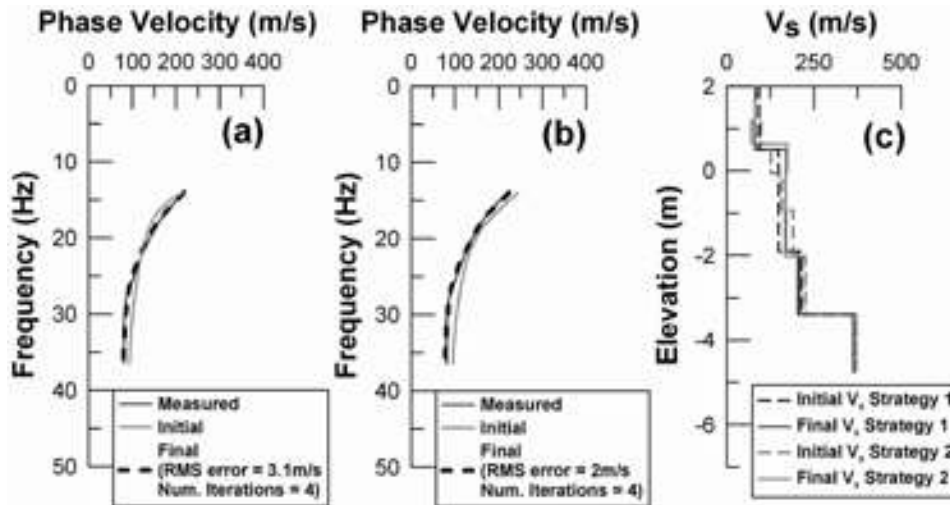


FIGURE 11

Measured, initial and final dispersion curves with associated errors for MASW 4, located on the natural ground to the east of the embankment, using a) inversion strategy 1 and b) inversion strategy 2 and c) initial and final inverted MASW V_s profiles for MASW 4.



FIGURE 12

Results of oedometer tests performed on samples of the soft alluvial clay deposit.

of boreholes 3 and 4 (Fig. 3). A trench of 1–2 m depth was excavated in this area and undisturbed samples were obtained by pushing 100 mm diameter, thin-walled stainless steel sampling tubes into the soft clay. The cutting edge of the sampling tubes was bevelled to 5° in order to minimize sampling disturbance (see Donohue and Long 2010). The samples were subjected to both triaxial and oedometer testing in order to obtain both strength and compressibility properties for the soft clay.

Undrained triaxial compression tests revealed that the soft clay had an undrained strength (s_u) of 22 kPa. A simple stability analysis, which assumes the embankment is analogous to an infinite strip footing, suggests that the ultimate bearing capacity (q_{ult}) of the soft clay beneath the embankment was approximately 113 kPa (see equation (2)):

$$q_{ult} = 5.15 s_u = 5.14 \times 22 = 113 \text{ kPa} \quad (2)$$

Given the stress applied (q_{app}) to the soil by the (4 m high) remodelled embankment was estimated to be 88 kPa (from borehole logs and density tests), the factor of safety ($FOS = q_{ult}/q_{app}$) was approximately 1.28. Whilst this is not unusually low for an embankment, it should be noted that the FOS value is very sensitive to the s_u value obtained in the triaxial strength tests. Since a limited number of samples were available, the exact FOS value is uncertain. An FOS value of 1.28 does, however, indicate a high ratio of applied to ultimate resistance and suggests that settlement will occur.

Oedometer tests were performed to assess the one-dimensional consolidation characteristics of the soft clay layer. Time-settlement curves measured on samples of the soft clay are shown in Fig. 12. These revealed that:

- samples tested at applied stresses up to 44 kPa exhibited elastic, primary settlement that terminated less than 100 minutes after application of the load;
- the maximum stress applied in the oedometer tests of 88 kPa represents a test on the material beneath the full-height embankment.

In this case, however, the sample shows a significant increase in settlement when the time exceeded 100 minutes. This is indicative of longer term consolidation and secondary compression (creep). Clearly, the increased stress generated by the remodelling of the embankment would generate large deformations in the soft alluvial soils in this area.

CONCLUSIONS

This study presented the results of a combined geophysical and geotechnical investigation into the failure of a newly remodelled section of a 150-year old railway embankment in the south-east of Ireland. The newly constructed remodelled embankment section suffered a rotational failure after it was constructed to its full

height. The 150-year old embankment, which also had a long-term history of settlement problems, was studied using a combination of geophysical (GPR, ERT and MASW) and geotechnical methods. Using GPR, an increase in the thickness of the ballast layer was detected around the area of failure, suggesting that long-term reballasting of this part of the embankment had taken place to offset settlement. The embankment itself appeared to have been founded partly on a layer of soft clay, the extent of which was determined using ERT. Profiles of ERT and MASW, acquired along the embankment crest (parallel to the direction of the tracks), also identified steeply sloping bedrock close to the area of failure, with a corresponding thickening of the low resistivity embankment fill. This is likely to have contributed to the long-term settlement problems encountered at this location. The small-strain shear stiffness (G_{\max}) of the embankment was also found to be low, using the MASW approach, indicating a soft embankment fill. This was also confirmed by boreholes drilled at the failure zone. It is likely that this material may have been softened due to rainfall infiltrating through the relatively high permeability ballast placed at the embankment crest and used to construct the side slopes of the remodelled embankment section.

The stratification identified by the geotechnical and geophysical investigations revealed the presence of a significant depth of low strength, high-compressibility soft clay under the area in which the remodelled embankment was constructed and this is thought to have been the major cause of this failure. Laboratory tests revealed that significant settlements in this deposit would be induced by these works. It is thought that hand construction of the original embankment took place over a much longer time period, thus allowing consolidation of the soft clay layer with associated strength gain during construction (analogous to modern stage construction techniques). Construction of the remodelled embankment is likely to have been too rapid as the extent of the soft clay zone was not known prior to construction.

Overall, the combination of traditional geotechnical and geophysical investigations was shown to provide key insights into the complex geological stratification beneath an old railway embankment. The results of this investigation were critical to understanding the cause of long-term settlement problems and recent stability problems affecting the remodelled embankment.

ACKNOWLEDGEMENTS

The work described in this paper is part of a research project with Iarnród Éireann, although the views expressed are those of the authors alone. The authors wish to thank Apex Geoservices and in particular Mr Peter O'Connor and Mr Andrew Trafford for their considerable assistance and also Mr Stephen Concannon and Mr Edward Conlan for their help on site. The first author would like to thank Pierse Contracting Ltd for their funding.

REFERENCES

Bogoslovsky V.A. and Ogilvy A.A. 1977. Geophysical methods for the investigation of landslides. *Geophysics* **42**, 562–571.

- Caris J.P.T. and Van Asch T.W.J. 1991. Geophysical, geotechnical and hydrological investigations of a small landslide in the French Alps. *Engineering Geology* **21**, 249–276.
- Carpenter D., Jackson P.J. and Jay A. 2004. Enhancement of the GPR method of railway trackbed investigation by the installation of radar detectable geosynthetics. *NDT&E International* **37**, 95–103.
- Cercato M. 2009. Addressing non-uniqueness in linearized multichannel surface wave inversion. *Geophysical Prospecting* **57**, 27–47.
- Cosentino P., Martorana R., Perniciaro M. and Terranova L.M. 2003. Geophysical study of a landslide in northern Sicily. *Near Surface Geophysics* **1**, 77–84.
- Deidda G.P. and Ranieri G. 2005. Seismic tomography imaging of an unstable embankment. *Engineering Geology* **82**, 32–42.
- Doherty P., Casey P. and Gavin K. 2006. Suitability of Macamore clay as an embankment fill and the role of soil suction in embankment stability. 3rd National Bridge and Transportation Infrastructure Symposium, 12–13 October, Expanded Abstracts.
- Donohue S., Gavin K., Long M. and O'Connor P. 2003. G_{\max} from multichannel analysis of surface waves for Dublin boulder clay. 13th European Conference on Soil Mechanics and Geotechnical Engineering (ECSMGE), Prague, Czech Republic, Expanded Abstracts, 515–520.
- Donohue S. and Long M. 2008. An assessment of the MASW technique incorporating discrete particle modelling. *Journal of Environmental and Engineering Geophysics* **13**, 57–68.
- Donohue S. and Long M. 2010. Assessment of sample quality in soft clay using shear wave velocity and suction measurements. *Géotechnique*. doi: 10.1680/geot.8.T.007.3741
- Donohue S., Long M., Gavin K. and O'Connor P. 2004. The use of multichannel analysis of surface waves in determining G_{\max} for soft clay. International Site Characterization 2 (ISC 2) Conference, Porto, Portugal, Expanded Abstracts, 459–466.
- Fourie A.B., Rowe D. and Blight G.E. 1999. The effect of infiltration on the stability of the slopes of a dry ash dump. *Géotechnique* **49**, 1–13.
- Friedel S., Thielen A. and Springman S.M. 2006. Investigation of a slope endangered by rainfall-induced landslides using 3D resistivity tomography and geotechnical testing. *Journal of Applied Geophysics* **60**, 100–114.
- Gavin K., Cadogan D. and Twomey L. 2008. Axial resistance of CFA piles in Dublin boulder clay. *ICE Proceedings: Geotechnical Engineering* **161**, 171–180.
- Gavin K., Xue J.F. and Jennings P. 2006. Assessment of the effect of pore pressures on the behaviour of railway foundations. 12th Danube-European Conference on Geotechnical Engineering, Ljubljana, Slovenia, Expanded Abstracts.
- Godio A. and Bottino G. 2001. Electrical and electromagnetic investigation for landslide characterisation. *Physics and Chemistry of the Earth, Part C, Solar, Terrestrial & Planetary Science* **26**, 705–710.
- Göktürkler G., Balkaya C. and Erhan Z. 2008. Geophysical investigation of a landslide: The Altındağ landslide site, İzmir (western Turkey). *Journal of Applied Geophysics* **65**, 84–96.
- deGroot-Hedlin C. and Constable S. 1990. Occam's inversion to generate smooth, two-dimensional models from magnetotelluric data. *Geophysics* **55**, 1613–1624.
- Hack R. 2000. Geophysics for slope stability. *Survey in Geophysics* **21**, 423–448.
- Hugenschmidt J. 2000. Railway track inspection using GPR. *Journal of Applied Geophysics* **43**, 147–55.
- Hyslip J., Smith S., Olhoeft G. and Selig E. 2003. Assessment of railway track substructure condition using ground penetrating radar. Proceedings of the 2003 Annual Conference of AREMA, Chicago, Illinois, USA, Expanded Abstracts.

- Israil M. and Pachauri A.K. 2003. Geophysical characterization of a landslide site in the Himalayan foothill region. *Journal of Asian Earth Sciences* **22**, 253–263.
- Jack R. and Jackson P.J. 1999. Imaging attributes of railway track formation and ballast using ground penetrating radar. *NDT&E International* **32**, 457–462.
- Jongmans D. and Garambois S. 2007. Geophysical investigation of landslides: A review. *Bulletin de la Societe Geologique de France* **178**, 101–112.
- Kovacevic N., Potts D.M. and Vaughan P.R. 2001. Progressive failure in clay embankments due to seasonal climate changes. *Proceedings of the 15th International Conference on Soil Mechanics and Geotechnical Engineering*, Istanbul, Turkey, Expanded Abstracts, 2127–2130.
- Lapenna V., Lorenzo P., Perrone A., Piscitelli S., Sdao F. and Rizzo E. 2003. High-resolution geoelectrical tomographies in the study of the Giarossa landslide (southern Italy). *Bulletin of Engineering Geology and the Environment* **62**, 259–268.
- Loke M.H. and Barker R.D. 1996. Rapid least-squares inversion of apparent resistivity pseudosections by a quasi-Newton method. *Geophysical Prospecting* **44**, 131–152.
- Long M. and Menkiti C.O. 2007. Geotechnical properties of Dublin Boulder Clay. *Géotechnique* **57**, 595–611.
- Luke B. and Calderón-Macías C. 2007. Inversion of seismic surface wave data to resolve complex profiles. *Journal of Geotechnical and Geoenvironmental Engineering* **133**, 155–165.
- McCann D.M. and Forster A. 1990. Reconnaissance geophysical methods in landslide investigations. *Engineering Geology* **29**, 59–78.
- Mondal S.K., Sastry R.G., Pachauri A.K. and Gautam P.K. 2008. High resolution 2D electrical resistivity tomography to characterize active Naitwar Bazar landslide, Garhwal Himalaya, India. *Current Science* **94**, 871–875.
- Nazarian S. and Stokoe K.H. 1984. In situ shear wave velocities from spectral analysis of surface waves. *Proceedings of the 8th World Conference on Earthquake Engineering*, San Francisco, California, USA, Expanded Abstracts, 31–38.
- O'Connor P. 2001. Applied geophysical methods in geotechnical investigations. *Proceedings of the 1st Geophysical Association of Ireland Seminar on Effective Use of Geophysical Methods in Ground Investigation*, Dublin, Ireland, Expanded Abstracts.
- Park C.B., Miller D.M. and Xia J. 1999. Multichannel Analysis of surface waves. *Geophysics* **64**, 800–808.
- Park C.B., Xia J. and Miller R.D. 1998. Imaging dispersion curves of surface waves on multichannel record. 68th SEG meeting, New Orleans, Louisiana, USA, Expanded Abstracts, 1377–1380.
- Rix G.J. and Stokoe K.H. 1988. In-situ seismic testing of landslide debris in Valtellina, Italy using surface waves. 58th SEG meeting, Anaheim, California, USA, Expanded Abstracts, 280–282.
- Sahbi H., Jongmans D. and Charlier R. 1997. Theoretical study of slope effects in resistivity surveys and applications. *Geophysical Prospecting* **45**, 795–808.
- Schmutz M., Albouy Y., Gurin R., Maquaire O., Vassal J., Schott J.-J. and Desclores M. 2000. Joint electrical and time domain electromagnetism (TDEM) data inversion applied to the super sauze earthflow (France). *Surveys in Geophysics* **21**, 371–390.
- Sjodahl P., Dahlin T. and Zhou B. 2006. 2.5D resistivity modeling of embankment dams to assess influence from geometry and material properties. *Geophysics* **71**, G107–G114.
- Suzuki K. and Higashi S. 2001. Groundwater flow after heavy rain in landslide-slope area from 2-D inversion of resistivity monitoring data. *Geophysics* **66**, 733–743.
- Xia J., Miller R.D. and Park C.B. 1999. Estimation of near surface shear wave velocity by inversion of Raleigh waves. *Geophysics* **64**, 691–700.
- Xue J.F. 2006. *Reliability analysis and the simulation of rainfall infiltration into partly saturated slopes*. PhD thesis, University College Dublin.